Catalysis Today xxx (2013) xxx–xxx

Contents lists available at ScienceDirect

Catalysis Today

journal homepage: www.elsevier.com/locate/cattod

Catalytic behaviour of a bifunctional system for the one step synthesis of DME by CO_2 hydrogenation

G. Bonura [a], M. Cordaro [b], C. Cannilla [a], A. Mezzapica [a], L. Spadaro [a], F. Arena [b], F. Frusteri [a],*

[a] CNR-ITAE, Istituto di Tecnologie Avanzate per l'Energia "Nicola Giordano", Via S. Lucia sopra Contesse, 5, 98126 Messina, Italy
[b] Dip. di Ingegneria Elettronica, Chimica e Ingegneria Industriale, Università di Messina, V.le F. Stagno D'Alcontres, 31, 98166 Messina, Italy

ARTICLE INFO

Article history:
Received 10 July 2013
Received in revised form 24 October 2013
Accepted 11 November 2013
Available online xxx

Keywords:
CO_2 hydrogenation
DME synthesis
Cu–ZnO–ZrO_2 catalysts
HZSM-5
Bifunctional catalysts

ABSTRACT

One-step CO_2 hydrogenation reaction to dimethyl ether (DME) on a bifunctional system constituted by Cu–ZnO–ZrO_2 (ZCZ) methanol synthesis catalyst and HZSM-5 zeolite was studied. The influence of the reactor configuration in terms of combination procedure of the admixed samples on activity, selectivity and DME yield has been evaluated. The results obtained at $T_R = 513$ K, $P_R = 3.0$ MPa and GHSV = 9000 $NL\,g_{cat}^{-1}\,h^{-1}$ show a superior DME productivity (4.4 mmol $kg_{ZCZ}^{-1}\,s^{-1}$) using the bifunctional catalyst prepared by physical mixing. A combined effect of active sites located at metal/oxide(s)–acid interface was claimed as the main factor affecting the CO_2 conversion and DME productivity. The strong surface acidity of ZCZ catalyst is not suitable to drive DME synthesis through a consecutive mechanism, while DME formation effectively proceeds on weak and medium acid sites of HZSM-5.

1. Introduction

The direct conversion of carbon dioxide into useful chemicals, like methanol (MeOH) and/or dimethyl ether (DME), is an attractive way of recycling CO_2 and thereby controlling its emission into the atmosphere [1–5]. In particular, DME is considered a prospective "future fuel" as a diesel substitute, due to its high cetane number [5,6]. In comparison to other synthetic fuels, DME has a very high thermal efficiency of combustion, equivalent to that of traditional fuels. It also does not emit sulphur oxides or soot and there is a considerable reduction of nitrous oxides in the exhaust gases. DME can be used as fuel for diesel engines as a cooking gas for household applications and running turbines in a power generation facility. Furthermore, DME can also be used as a starting material for the production of a range of chemicals, such as oxygenates, olefins, and hydrocarbon fuels (gasoline, jet fuel) or as an efficient H_2 carrier for fuel cells and other applications [5–7].

Notwithstanding an extensive literature documents the feasibility of a process for the production of DME *via* syngas [8–19], only few papers deal with the DME synthesis *via* CO_2 hydrogenation [5,20–29]:

$$CO_2 + 6H_2 \leftrightharpoons CH_3OCH_3 + 3H_2O \quad \Delta H_{298} = -122.2\,\text{KJ mol}^{-1} \qquad (1)$$

Fundamentally, there are two routes for the production of DME: (i) a two-steps process, in which methanol is first produced on a metallic catalyst and then dehydrated to DME on an acid catalyst located in a second reactor [30–32]; (ii) a single step process, in which bifunctional catalysts constituted by metallic and acidic functionalities are used in only one reactor to perform the reactions simultaneously [30–32]. The main advantage of the single-step process is the elimination of thermodynamic restriction of methanol synthesis. Whichever is the approach, two consecutive steps or one single step, three independent reactions are always involved in the DME synthesis process from CO_2/H_2 mixtures, being other possible reactions easily obtained by linear combination of the followings:

Methanol synthesis reaction (MS):

$$CO_2 + 3H_2 \leftrightharpoons CH_3OH + H_2O \quad \Delta H^\circ = -49.4\,\text{KJ mol}^{-1} \qquad (2)$$

Methanol dehydration reaction (MD):

$$2CH_3OH \leftrightharpoons CH_3OCH_3 + H_2O \quad \Delta H^\circ = -23.4\,\text{KJ mol}^{-1} \qquad (3)$$

Reverse water gas shift reaction (RWGS):

$$CO_2 + H_2 \leftrightharpoons CO + H_2O \quad \Delta H^\circ = +41.2\,\text{KJ mol}^{-1} \qquad (4)$$

Catalysts for the direct CO_2-to-DME process should be able to efficiently catalyse both MS and MD reactions, while the yield of CO, formed *via* the RWGS side reaction [27,33], should be kept to a minimum.

Typically, MS reaction is carried out on Cu–ZnO–Al_2O_3 catalysts, although Cu–ZnO–ZrO_2 catalysts are recently claimed as more active catalytic systems due to a better water tolerance of zirconia

---

* Corresponding author.
E-mail address: francesco.frusteri@itae.cnr.it (F. Frusteri).

0920-5861/$ – see front matter © 2013 Elsevier B.V. All rights reserved.
http://dx.doi.org/10.1016/j.cattod.2013.11.017

Table 1
Physicochemical characteristics of ZCZ catalyst.

CuO (wt.%)	41.2
ZnO (wt.%)	14.8
ZrO_2 (wt.%)	44.0
Surface area ($m^2\,g^{-1}$)	174 ± 1
Pore volume ($cm^3\,g^{-1}$)	0.310
Copper specific area[a] ($m^2\,g^{-1}$)	60.8
Copper dispersion[a] (%)	29.1
Copper crystallite size[a] (nm)	4

[a] From "single-pulse" (363 K) N_2O titration measurements (see Ref. [37]).

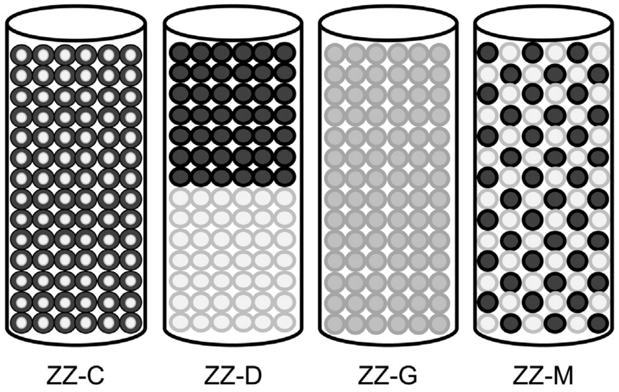

Fig. 1. Combination procedures between methanol and acid catalyst (● ZCZ; ○ HZSM-5).

in respect of alumina [34–37]. MD reaction, instead, fast takes place over a solid acid component.

In the present work, a Cu–ZnO–ZrO_2 catalyst and a mesoporous HZSM-5 zeolite are used as methanol synthesis and dehydration component, respectively. Although mesoporous zeolites suffer from a lack of size and shape selectivity, contrarily to microporous zeolites, their use have been proved to exhibit better activity and higher resistance to deactivation due to hierarchical structure, which improves the mass transfer process during the reactions [38–40]. Four different combination procedures between the two components have been adopted, in order to maximize the contact between CO_2 activation, hydrogenation and methanol dehydration sites. The influence of the preparation method in the one step synthesis of DME by CO_2 hydrogenation is discussed.

2. Experimental

2.1. Catalyst preparation

The Cu–ZnO–ZrO_2 (ZCZ) methanol synthesis catalyst, with a Zn/Cu atomic ratio of 0.4, was prepared by "reverse co-precipitation method under ultrasound irradiation", according to the procedure elsewhere reported [37]. The list of physicochemical properties of such a catalyst is reported in Table 1.

To form the bifunctional system, the ZCZ catalyst was admixed to a commercial mesoporous NH_4-ZSM-5 zeolite (Zeolyst Int. CBV3024E), characterized by a SiO_2/Al_2O_3 molar ratio of 30. The zeolite was converted in its protonic form by calcination in air at 773 K (SA_{BET}, 317 $m^2\,g^{-1}$; PV_{meso}, 0.200 $cm^3\,g^{-1}$; PV_{micro}, 0.115 $cm^3\,g^{-1}$). Considering that previous results dealing with the influence of zeolite loading on a hybrid catalyst shed light on an optimal ratio of 1:1 (w/w) between methanol synthesis catalyst and zeolite [33], four different combination procedures (see Fig. 1) were adopted to get a bifunctional system, as follows:

(1) ZZ-C, reverse co-precipitation of ZCZ metallic precursors under ultrasound irradiation in a pH 8 buffered solution containing an appropriate amount of HZSM-5 finely dispersed, under vigorous stirring in an ultrasound bath maintained at 310 K. The hybrid catalyst was dried at 383 K for 16 h and further calcined at 623 K for 4 h. Then, the sample was crushed and sieved and the 40–70 mesh particle size fraction was used for characterization and testing measurements;
(2) ZZ-D, dual-bed of same-sized (40–70 mesh) ZCZ methanol catalyst (first bed) and HZSM-5 catalyst (second bed);
(3) ZZ-G, homogeneous solid mixture, prepared by grinding in an agate mortar of powdered single catalysts and pelletization (40–70 mesh) of the resulting bifunctional system; and
(4) ZZ-M, homogeneous physical mixture of same-sized (40–70 mesh) ZCZ and HZSM-5 catalysts.

2.2. Catalysts characterization

Surface area (SA) and pore volume (PV). Nitrogen adsorption/desorption isotherms for SA and PV calculations were obtained by using a Micromeritics ASAP 2020 gas adsorption device. Before analysis, all the samples were outgassed at 453 K under vacuum (3 h).

X-ray diffraction (XRD) analyses of the samples in the 2θ range 5–100° were performed using a Philips X-Pert diffractometer, operating with Ni β-filtered Cu Kα radiation (λ = 1.5406 Å) at 40 kV and 30 mA and a scan step of 0.05° s^{-1}. Identification of XRD patterns was made on the basis of the JCPDS database [41].

Ammonia temperature programmed desorption (NH_3-TPD). NH_3-TPD measurements in the range 373–973 K were performed in a conventional flow apparatus by using *ca.* 100 mg sample in a linear quartz micro-reactor (*i.d.*, 4 mm; *l.*, 200 mm), with a helium carrier flow rate of 25 *STP* mL min^{-1}. Prior to each measurement, the sample was pretreated at 573 K with hydrogen flowing at 100 mL min^{-1} for 1 h and then cooled down to 423 K and saturated at a flow rate of 25 mL min^{-1} for 1.5 h with a 5% NH_3/He stream. Then, the samples were purged in He atmosphere for *ca.* 1 h until baseline stabilization.

Transmission electron microscopy (TEM) analysis. A *Philips CM12* instrument equipped with a high-resolution camera was used to acquire and elaborate TEM images. Powdered samples were dispersed in 2-propanol under ultrasound irradiation and the resulting suspension put drop-wise on a holey carbon-coated support grid.

2.3. Catalyst testing

Catalyst testing was performed in a fixed-bed stainless steel reactor (*i.d.*, 4 mm; *l.*, 200 mm), loaded with 0.25 g of hybrid catalyst, diluted with inert same-sized SiC (0.25 g). A $CO_2/H_2/N_2$ reaction mixture with a molar ratio of 23/69/8 was fed at a temperature ranging from 443 to 563 K, pressure of 0.1–5.0 MPa and gas hourly space velocity (GHSV) between 4500 and 36,000 *NL* $kg_{cat}^{-1}\,h^{-1}$. Prior to each test, the catalyst was reduced *in situ* at 573 K for 1 h in pure hydrogen flow at atmospheric pressure. The reaction stream was analysed by a GC equipped with a two-column separation system connected to a flame ionized detector and thermal conductivity detector, respectively. CO_2 conversion along with DME, MeOH and CO selectivity were obtained from the GC data and calculated as elsewhere reported [33].

3. Results and discussion

3.1. Textural properties

According to previous evidences on the optimum composition of the methanol Cu–ZnO–ZrO_2 system [37], it was seen that a high content of hydrophobic zirconia carrier (≈44 wt.%) promotes

Please cite this article in press as: G. Bonura, et al., Catalytic behaviour of a bifunctional system for the one step synthesis of DME by CO_2 hydrogenation, Catal. Today (2013), http://dx.doi.org/10.1016/j.cattod.2013.11.017

Table 2
Textural properties of the investigated bifunctional catalysts.

Sample	SA ($m^2\,g^{-1}$)	PV ($cm^3\,g^{-1}$)	APD[b] (Å)
ZZ-C	251	0.266	42
ZZ-G	223	0.173	31
ZZ-M[a]	245	0.313	51

[a] Averaged values between ZCZ and H-ZSM5 samples.
[b] Average pore diameter (APD, 4PV/SA).

structure and texture (see Table 1), enhancing the activity of the Cu–ZnO based system in the presence of water [42]. Moreover, synergistic effects of the ZrO_2 carrier and ZnO promoter on Cu exposure determine a significantly high dispersion (29%) and MSA ($60.8\,m^2\,g^{-1}$) of the ZCZ system, as a consequence of high surface area ($174\,m^2\,g^{-1}$) induced by the use of the reverse co-precipitation procedure under ultrasound irradiation [36].

Table 2 shows the physicochemical properties of the prepared bifunctional systems. The co-precipitated ZZ-C sample exhibits textural properties similar to ZZ-M, that is the system obtained by physical mixing of ZCZ catalyst and HZMS-5 zeolite. In particular, ZZ-C presents *SA* of $251\,m^2\,g^{-1}$, very close to *SA* of ZZ-M ($245\,m^2\,g^{-1}$), the value of which was calculated as an average between ZCZ and HZSM-5 samples. Instead, lower *SA* ($223\,m^2\,g^{-1}$) value is recorded for the ZZ-G sample, as a consequence of the grinding procedure of the admixed catalysts that causes a porosity shrinkage (*PV*, $0.173\,cm^3\,g^{-1}$), with a decreasing of *APD* to 31 Å. Then, the decrease in *SA* and *PV* observed for such catalyst should be mostly attributed to a pore blockage of the zeolite mesopores by Cu–ZnO–ZrO_2 particles [1].

3.2. Structural properties

Fig. 2 shows XRD patterns of methanol synthesis catalyst (ZCZ), dehydration catalyst (HZSM-5) and bifunctional systems (ZZ-C and ZZ-G). As it is possible to observe, ZCZ exhibits an amorphous pattern with a lack of "long range" crystalline order, which accounts for the formation of nanosized oxide domains [36,37], in which a high copper dispersion (29%) reflects copper crystallite size of 4 nm (see Table 1). On the other hand, in the bifunctional Cu–ZnO–ZrO_2/HZSM-5 systems, the characteristic reflections of HZSM-5 zeolite (JPCDS 44-0002) are always present, independently of different catalyst preparation methods employed. Furthermore, ZZ-C system shows an amorphous pattern in the 2θ range of 25–40°, similar to that observed in the "bare" ZCZ, which signals high dispersion of methanol synthesis catalyst on the zeolite matrix. On the contrary, ZZ-G system shows two little signals at 35.4° and 38.7°, ascribable to diffraction planes $\langle -1\,1\,1 \rangle$ and $\langle 1\,1\,1 \rangle$ of the crystalline tenorite CuO phase (JPCDS 5-661). By Scherrer's equation applied to the $\langle -1\,1\,1 \rangle$ line, a mean CuO crystallite size of 6.2 nm was obtained, diagnostic of a significant increase of CuO particle size upon the grinding procedure. Such findings are confirmed by TEM analysis of the studied samples, as shown in Fig. 3. Indeed, in the ZZ-G catalyst, isolated metallic copper particles are randomly distributed over zeolite matrix, missing the typical cluster structure of the ZCZ catalyst. As previously reported [33], this is the result of a mechanical stress induced by grinding procedure, which determines a detrimental interaction between the two functionalities (ZCZ and HZSM-5). On the contrary, the co-precipitated ZZ-C sample also shows highly dispersed metal-oxide(s) particles on zeolite matrix, with a rather uniform size distribution. ZZ-M, being a combination of the two mechanically mixed functionalities, merely features the isolated structure of methanol ZCZ catalyst and HZSM-5 zeolite, without any evidence of intimate chemical interaction.

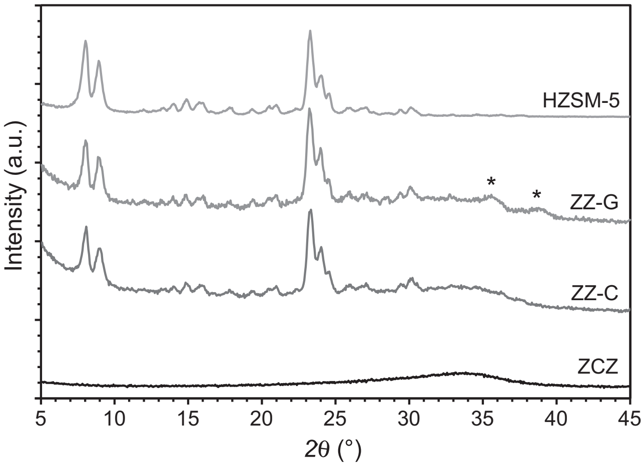

Fig. 2. XRD patterns of methanol synthesis catalyst (ZCZ), methanol dehydration catalyst (HZSM-5) and bifunctional catalysts (ZZ-C and ZZ-G).

3.3. Surface properties

As known, although by NH_3-TPD measurements is not possible to discriminate between Brønsted and Lewis acidity, ammonia desorbed as a function of temperature can give a reliable measure of acid strength. As reported in Table 3, ZCZ is characterized by a low adsorption capacity ($0.38\,mmol\,NH_3\,g_{cat}{}^{-1}$), totally associated to ammonia desorbed at high temperature (T_d, 823 K) from strong acid sites. Instead, the acid distribution of the HZSM-5 zeolite is the result of weak (27%) and medium acid sites (73%) spanned in the range 506–685 K, with a cumulative amount of desorbed ammonia of $0.88\,mmol\,g_{cat}{}^{-1}$.

All bifunctional systems show similar adsorption capacity ($1.01–1.20\,mmol\,NH_3\,g_{cat}{}^{-1}$), with a far higher number of acid sites than the pure materials. This is likely caused by the water formed during catalyst activation/reduction that induces dealumination phenomena on zeolite, so increasing the total acidity of the systems [43–45]. As also displayed in Fig. 4, both ZZ-M and ZZ-D samples exhibit a low concentration of weak sites (14–19%) and an overall population of medium and strong sites of 81% and 86%, respectively. In spite of a similar surface acidity ($1.06\,mmol\,g_{cat}{}^{-1}$), the

Table 3
Quantitative data of NH_3-TPD patterns and acid sites distribution.[a]

Sample	Amount desorbed ($mmol\,g_{cat}{}^{-1}$)	Weak sites		Medium sites		Strong sites	
		T_{d1} (K)	x_1	T_{d2} (K)	x_2	T_{d3} (K)	x_3
ZCZ	0.38	–	–	–	–	823	1.00
ZZ-C	0.37	–	–	636	0.18	826	0.82
ZZ-D	1.20	506	0.14	676	0.60	823	0.26
ZZ-G	1.06	498	0.34	695	0.27	857	0.39
ZZ-M	1.01	505	0.19	684	0.49	824	0.32
HZSM-5	0.88	506	0.27	685	0.73	–	–

[a] T_{dn}, temperature of desorption maximum; x_n, fractional population of sites.

Please cite this article in press as: G. Bonura, et al., Catalytic behaviour of a bifunctional system for the one step synthesis of DME by CO_2 hydrogenation, Catal. Today (2013), http://dx.doi.org/10.1016/j.cattod.2013.11.017

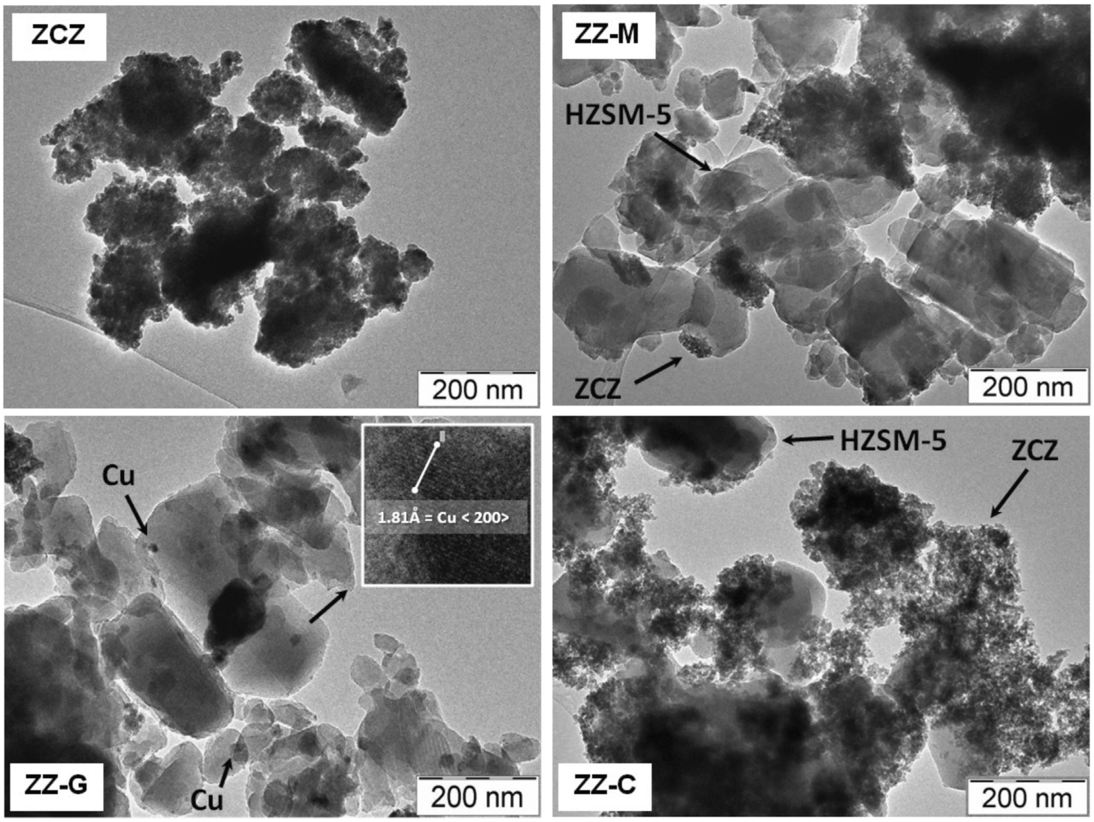

Fig. 3. TEM micrographs of the prepared bifunctional catalysts.

ZZ-G sample features a more balanced distribution of acid sites in the range of temperature investigated, with a homogenization of sites having different strength ($0.27 < x_n < 0.39$) with respect to the other systems. At last, with a fairly low amount of ammonia desorbed (0.37 mmol NH_3 $g_{cat}{}^{-1}$), the ZZ-C catalyst outlines the predominance of strong acid sites (82%) and only a little population of medium sites (18%), without any appearance of weaker acid sites at low temperature. Evidently, the co-precipitation of ZCZ in an aqueous medium in which HZSM-5 was dispersed caused a loss of weak-medium acidity of zeolite, accounting for an almost complete (82%) fraction of NH_3 retained above 673 K.

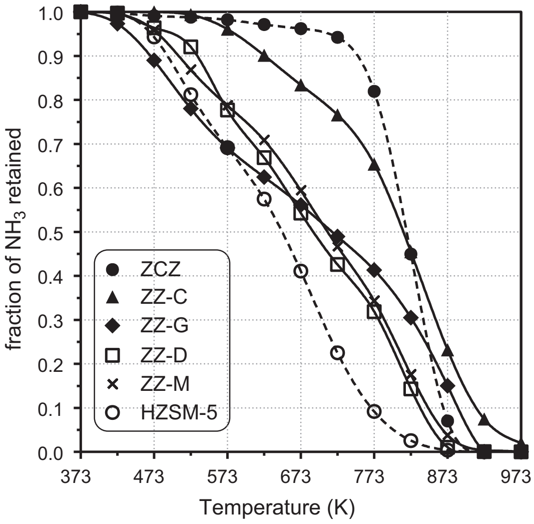

Fig. 4. Fraction of ammonia retained on catalyst surface as a function of evacuation temperature.

3.4. Catalytic results

Initially, the effect of the preparation method of the $CuO–ZnO–ZrO_2$/HZSM-5 bifunctional systems on CO_2 conversion and MeOH/DME formation rates was studied. Fig. 5 shows the results obtained at 513 K, 3.0 MPa and space velocity of 9000 *NL* $kg_{cat}{}^{-1}$ h^{-1}. As a reference, the activity pattern of the

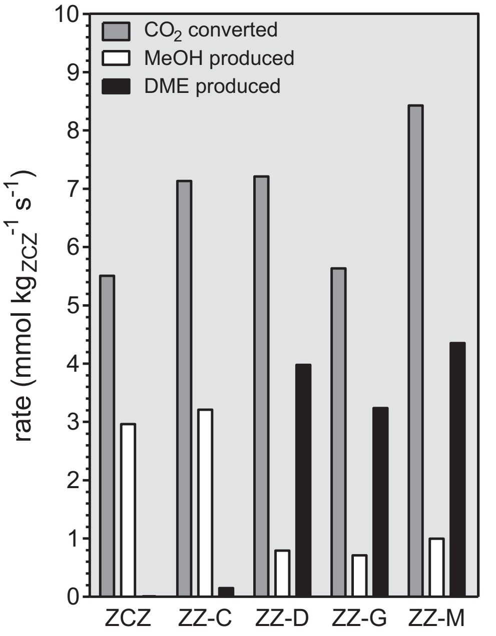

Fig. 5. Influence of mixing methodology on the reaction rate (T_R, 513 K; P_R, 3.0 MPa; GHSV, 9000 *NL* $kg_{cat}{}^{-1}$ h^{-1}).

Please cite this article in press as: G. Bonura, et al., Catalytic behaviour of a bifunctional system for the one step synthesis of DME by CO_2 hydrogenation, Catal. Today (2013), http://dx.doi.org/10.1016/j.cattod.2013.11.017

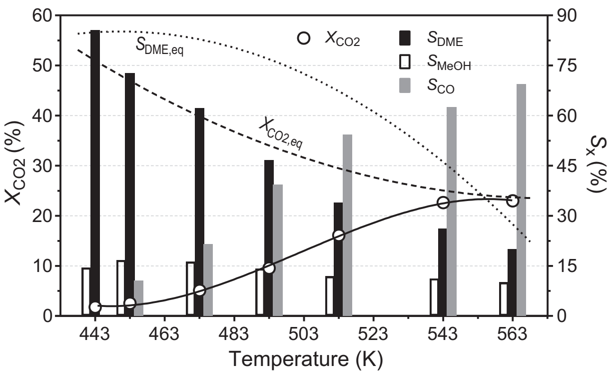

Fig. 6. Influence of reaction temperature. Catalyst: ZZ-M (P_R, 3.0 MPa; GHSV, 9000 *NL* kg_{cat}^{-1} h^{-1}). Dotted lines refer to equilibrium values of CO_2 conversion (—) and DME selectivity (···).

ZCZ methanol catalyst is also reported. No hydrocarbons or coke were found under the adopted experimental conditions. Notwithstanding the presence of strong acid sites evidenced by NH_3-TPD measurements, the rate of DME production on ZCZ is close to zero. On the whole, the ZZ-M catalyst presents the highest rate, both in terms of CO_2 conversion (8.4 mmol kg_{ZCZ}^{-1} s^{-1}) and DME production (4.4 mmol kg_{ZCZ}^{-1} s^{-1}), in consequence of faster mass transfer phenomena occurring between neighbouring metal/oxide(s)–acid sites, so favouring the shifting of methanol equilibrium towards DME with an increased CO_2 conversion. Instead, the dual bed ZZ-D system, in which methanol formed in the first step on ZCZ is converted into DME on acid sites of zeolite in the second step, attains only an enhancement of CO_2 conversion rate over 20% with respect to the reference system, without reaching the productivity of the ZZ-M catalyst. Similarly to ZZ-D, an interesting CO_2 conversion value was observed on the ZZ-C sample, prepared by co-precipitation of metallic precursors on powdered zeolite. Nevertheless, a quasi-zero DME production was achieved on such a system, due to a surface acidity too strong, not suitable to effectively drive the dehydration of methanol to DME [33]. Indeed, the disappearance of weak-medium acid sites of zeolite is likely due to the preparation method that, during the co-precipitation step, causes an ionic exchange of acid sites of zeolite with metal precursors of ZCZ catalyst. At last, although the attempt to realize a more intimate contact between metal/oxide(s) and acid sites at interface, the ZZ-G sample exhibits a lower CO_2 conversion and DME production (3.2 mmol kg_{ZCZ}^{-1} s^{-1}), being ascribable to a mechanical stress induced by grinding in mortar of the two admixed catalysts (ZCZ and HZSM-5) that caused a detrimental interaction among the active sites [33].

Considering the interesting result obtained over the ZZ-M sample, the influence of experimental conditions on CO_2 conversion (X_{CO_2}) and product selectivity (S_x) was studied on such a system in more detail, in terms of reaction temperature, reaction pressure, space velocity and catalyst particle size, as shown in Figs. 6–9.

Thermodynamically, being an exothermic reaction, it is easier to synthesize DME from CO_2 at low reaction temperature (see reaction (1)). So, the activity–selectivity pattern in a range of reaction temperatures between 443 and 563 K was studied. At 3.0 MPa and flow rate of 9000 *NL* kg_{cat}^{-1} h^{-1} (Fig. 6), the CO_2 conversion increases from 1.9% to 23.0%, until reaching a plateau at higher temperature (543–563 K), in correspondence of the thermodynamic equilibrium. On the other hand, DME selectivity shows a decreasing trend with reaction temperature, from a maximum of 86% at 443 K up to a minimum value of 20% at 563 K. On the contrary, CO selectivity rapidly increases with reaction temperature, attaining a maximum value of 69% at 563 K. Indeed, such a significant CO production at higher temperature is mainly ascribable to a prevailing contribution of the reverse water gas shift (RWGS) reaction [33], which is an endothermic process (see reaction (4)). Moreover, MeOH selectivity maintains an almost constant level (12–17%) along the investigated temperature range, as the result of the competition between exothermic MS and MD reactions (reactions (2) and (3)).

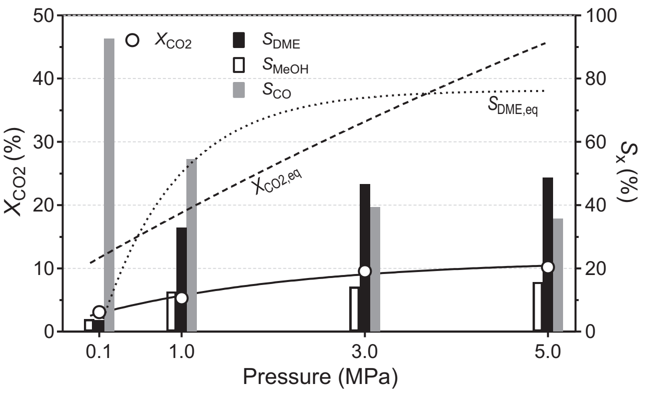

Fig. 7. Influence of reaction pressure. Catalyst: ZZ-M (T_R, 493 K; GHSV, 9000 *NL* kg_{cat}^{-1} h^{-1}). Dotted lines refer to equilibrium values of CO_2 conversion (—) and DME selectivity (···).

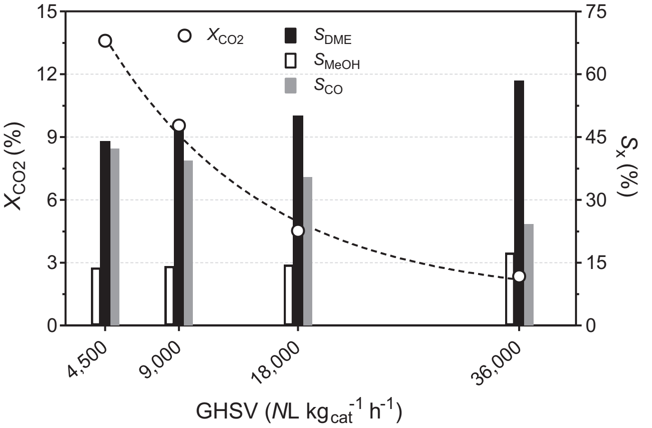

Fig. 8. Influence of space velocity. Catalyst: ZZ-M (T_R, 493 K; P_R, 3.0 MPa).

As regards the influence of reaction pressure on catalytic activity, experiments carried out at 493 K and 9000 *NL* kg_{cat}^{-1} h^{-1} are shown in Fig. 7. As it is possible to observe, the CO_2 conversion only slightly increases with pressure, from 3.1% (at P_R, 0.1 MPa) to

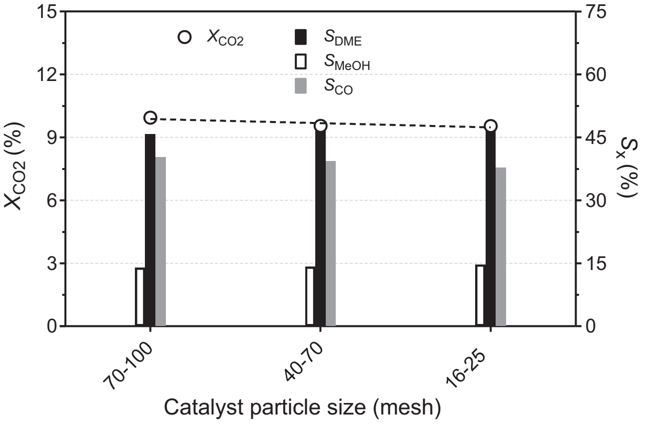

Fig. 9. Influence of catalyst particle size. Catalyst: ZZ-M (T_R, 493 K; P_R, 3.0 MPa; GHSV, 9000 *NL* kg_{cat}^{-1} h^{-1}).

Please cite this article in press as: G. Bonura, et al., Catalytic behaviour of a bifunctional system for the one step synthesis of DME by CO_2 hydrogenation, Catal. Today (2013), http://dx.doi.org/10.1016/j.cattod.2013.11.017

10.2% (at P_R, 5.0 MPa), without any significant improvement from 3.0 to 5.0 MPa. So, it is confirmed that, being a molar decreasing reaction (see reaction (1)), DME synthesis by CO_2 hydrogenation is favoured as the pressure increases. Moreover, at atmospheric pressure CO represents the main product, with a selectivity of 92.5% which rapidly decreases with pressure until to reach a value of 35.7% at 5.0 MPa. On the contrary, as also expected from thermodynamic predictions, the DME formation takes advantage of pressure increasing and selectivity reaches the maximum value of 48.6% at 5.0 MPa. Nevertheless, the MeOH selectivity also increases with pressure, although the values do not exceed 15.7% under the investigated experimental conditions. Indeed, since both MD and RWGS reactions are only slightly affected (if at all) by a rise in pressure (according to the negligible volume variation of reactions (3) and (4)), a lower dependence of CO_2 conversion on high-pressure conditions ($P_R > 3.0$ MPa) likely reflects a more extensive wetting of the catalyst surface, in consequence of the partial pressure of water which, rising with conversion and pressure, causes an incipient oxidation of Cu sites depressing the catalyst activity [36,37].

Considering that the reaction under investigation is characterized by multiple (parallel and/or consecutive) reaction paths [33], occurring on different surface active sites (metal/oxide(s)–acid) at different reaction rates, experiments at different flow rates have been performed with the aim to optimize the yield to DME production. In this respect, the effect of space velocity on the activity–selectivity pattern of the ZZ-M catalyst was investigated by operating at T_R, 493 K and P_R, 3.0 MPa. As shown in Fig. 8, between 4500 and 36,000 *NL* kg_{cat}^{-1} h^{-1}, a regular decreasing in CO_2 conversion from 13.6% to 2.4% is observed, while, in terms of selectivity, a progressive increase of DME production, from 42% to 59%, is recorded. On the contrary, CO selectivity decreases from 42% to 24%, while the MeOH selectivity shows only a slight variation (14–19%) in the whole range of space velocity investigated. Since at low flow rates the occurrence of external mass transfer constraints begins to be evident, operation at a space velocity of 9000 *NL* kg_{cat}^{-1} h^{-1} is resulted suitable to enhance the mass transfer phenomena [46].

Moreover, as the reaction takes place over a bifunctional system, which also involves an intraphase mass transfer among different sites, the effect of catalyst particle size on CO_2 conversion and product selectivity (see Fig. 9) has been also investigated. Ranging from 70–100 to 16–25 mesh, in all tests performed no difference was observed either in terms of CO_2 conversion or products distribution. Based on these results, it is possible to draw that, under isothermal conditions, the internal mass transfer rate of methanol from metal-oxide(s) sites of ZCZ to the acid sites of HZSM-5 does not affect the activity–selectivity pattern, likely because the concentration profiles (of reactants and products) within the catalytic particle do not change with the grain size. In any case, the 40–70 mesh fraction was chosen for further investigations as the suitable compromise between the pressure drop along the reactor and the mechanical resistance of catalyst particle.

At last, in Fig. 10 the influence of the zeolite loading on the space-time yield of DME (STY) was also investigated. As it is possible to observe, the rate of DME production in the absence of zeolite results near to zero, clearly demonstrating that strong acid sites (totally associated to ZCZ, as seen in Table 2) are not suitable to promote the dehydration reaction of methanol to DME. On the other hand, no conversion of CO_2 was observed over the "bare" zeolite, because the lack of a specific functionality for CO_2 and H_2 activation. Overall, at any investigated reaction temperature, the specific DME productivity follows a volcano-shape trend with a maximum in correspondence of a zeolite loading of 50 wt.%.

Such a result clearly emphasizes that the catalytic behaviour of the Cu–ZnO–ZrO_2/HZSM-5 bifunctional catalyst is tightly dependent on the ratio between metal-oxide(s) and acid surface sites.

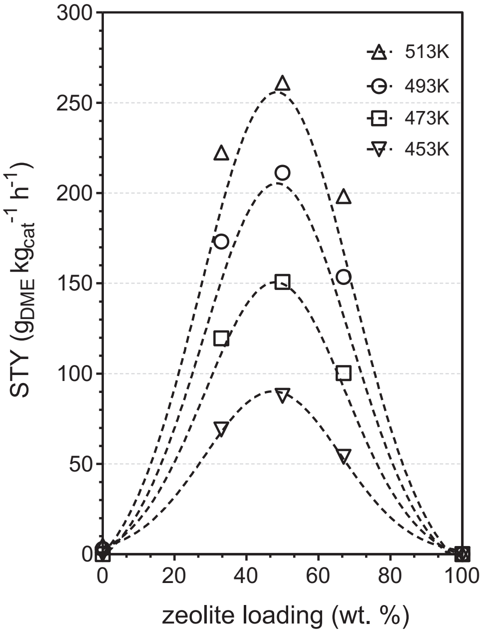

Fig. 10. Effect of zeolite loading on DME productivity at different reaction temperature (P_R, 3.0 MPa; GHSV, 9000 *NL* kg_{cat}^{-1} h^{-1}).

4. Conclusions

In the present study, the performance of a novel Cu–ZnO–ZrO_2/HZSM-5 catalytic formulation for the one-step DME production by CO_2 hydrogenation has been investigated.

Different combination procedures between methanol synthesis catalyst and methanol dehydration catalyst have been adopted, so obtaining bifunctional systems characterized by different textural, structural and surface properties.

Reaction temperature and pressure play a fundamental role in driving the reaction towards DME formation. According to thermodynamics, the DME formation is favoured at low temperature (<513 K), whereas at high pressure (>3.0 MPa) the negative role of water on catalyst activity is envisaged.

Catalytic data in the absence of zeolite disclose that strong acid sites of Cu–ZnO–ZrO_2 catalyst are not suitable for DME synthesis, while the bifunctional ZZ-M sample, prepared by physical mixing of the pre-pelletized catalysts, exhibits a superior performance with respect to the other investigated systems, mainly when a zeolite loading of 50 wt.% is used.

Acknowledgements

This work was financially supported by the Italian Research Fund (PON R&C 2007–2013, DD 713/Ric. 29.10.2010, PON02_00451_3362376) through the "BIO4BIO" project, Biomolecular and Energy valorization of residual biomass from Agroindustry and Fishing Industry.

The authors would like to thank the scientific advisory board of 10th Natural Gas Conversion Symposium 2013, Doha, Qatar, for the "First place Poster Award" received as an official acknowledgement for the results presented at the conference.

The authors also thank Prof. Girolamo Giordano and Dr. Alfredo Aloise from University of Calabria for performing the BET measurements.

References

[1] A. García-Trenco, A. Vidal-Moya, A. Martínez, Catal. Today 179 (2012) 43–51.
[2] N. Tsubaki, M. Ito, K. Fujimoto, J. Catal. 197 (2001) 224–227.

Please cite this article in press as: G. Bonura, et al., Catalytic behaviour of a bifunctional system for the one step synthesis of DME by CO_2 hydrogenation, Catal. Today (2013), http://dx.doi.org/10.1016/j.cattod.2013.11.017

[3] T. Sakakura, K. Kohno, Chem. Commun. (2009) 1312–1330.
[4] M. Mikkelsen, M. Jørgensen, F.C. Krebs, Energy Environ. Sci. 3 (2010) 43–81.
[5] W. Wang, S. Wang, X. Ma, J. Gong, Chem. Soc. Rev. 40 (2011) 3703–3727.
[6] T.A. Semelsberger, K.C. Ott, R.L. Borup, H.L. Greene, Appl. Catal. A 309 (2006) 210–223.
[7] M. Nilsson, L.J. Pettersson, B. Lindstrom, Energy Fuels 20 (2006) 2164–2169.
[8] V.M. Lebarbier, R.A. Dagle, L. Kovarik, J.A. Lizarazo-Adarme, D.L. King, D.R. Palo, Catal. Sci. Technol. 2 (2012) 2116–2127.
[9] J.W. Jung, Y.J. Lee, S.H. Um, P.J. Yoo, D.H. Lee, K.-W. Jun, J.W. Bae, Appl. Catal. B 126 (2012) 1–8.
[10] A. García-Trenco, A. Martínez, Appl. Catal. A 411–412 (2012) 170–179.
[11] J.H. Flores, D.P.B. Peixoto, L.G. Appel, R.R. De Avillez, M.I.P.D. Silva, Catal. Today 172 (2011) 218–225.
[12] S.-C. Baek, S.-H. Kang, J.W. Bae, Y.-J. Lee, D.-H. Lee, K.-Y. Lee, Energy Fuels 25 (2011) 2438–2443.
[13] Y. Luan, Adv. Mater. Res. 183–185 (2011) 1505–1508.
[14] J. Palgunadi, I. Yati, K.D. Jung, React. Kinet. Mech. Catal. 101 (2010) 117–128.
[15] P.S.S. Prasad, J.W. Bae, S.H. Kang, Y.J. Lee, K.W. Jun, Fuel Process. Technol. 89 (2008) 1281–1286.
[16] S.H. Kang, J.W. Bae, K.W. Jun, H.S. Potdar, Catal. Commun. 9 (2008) 2035–2039.
[17] K.S. Yoo, J.H. Kim, M.J. Park, S.J. Kim, O.S. Joo, K.D. Jung, Appl. Catal. A 330 (2007) 57–62.
[18] F.S. Ramos, A.M. Duarte de Farias, L.E.P. Borges, J.L. Monteiro, M.A. Fraga, E.F. Sousa-Aguiar, L.G. Appel, Catal. Today 101 (2005) 39–44.
[19] K. Sun, W. Lu, F. Qiu, S. Liu, X. Xu, Appl. Catal. A 252 (2003) 243–249.
[20] Q. Zhang, Y.-Z. Zuo, M.-H. Han, J.-F. Wang, Y. Jin, F. Wei, Catal. Today 150 (2010) 55–60.
[21] S. Wang, D. Mao, X. Guo, G. Wu, G. Lu, Catal. Commun. 10 (2009) 1367–1370.
[22] X. An, Y.Z. Zuo, Q. Zhang, D.Z. Wang, J.F. Wang, Ind. Eng. Chem. Res. 47 (2008) 6547–6554.
[23] J.-Y. Wang, X.-H. Wang, C.-Y. Zeng, C.-Z. Wu, Shiyou Xuebao Shiyou Jiagong/Acta Pet. Sin. (Pet. Process. Sect.) 23 (2007) 62–68.
[24] J.-Y. Wang, C.-Y. Zeng, C.-Z. Wu, J. Fuel Chem. Technol. 34 (2006) 195–199.
[25] J.-Y. Wang, C.-Y. Zeng, Xiandai Huagong/Mod. Chem. Ind. 26 (2006) 35–39.
[26] H.-W. Liu, D.-H. Liu, W.-Y. Ying, D.-Y. Fang, Gaoxiao Huaxue Gongcheng Xuebao/J. Chem. Eng. Chin. Univ. 19 (2005) 59–64.
[27] F. Arena, L. Spadaro, O. Di Blasi, G. Bonura, F. Frusteri, Stud. Surf. Sci. Catal. 147 (2004) 385–390.
[28] K. Sun, W. Lu, M. Wang, X. Xu, Catal. Commun. 5 (2004) 367–370.
[29] T. Tagawa, M. Ito, S. Goto, Appl. Organomet. Chem. 15 (2001) 105–108.
[30] D. Mao, W. Yang, J. Xia, B. Zhang, Q. Song, Q. Chen, J. Catal. 230 (2005) 140–149.
[31] D. Mao, W. Yang, J. Xia, B. Zhang, G. Lu, J. Mol. Catal. A: Chem. 250 (2006) 138–144.
[32] L. Wang, D. Fang, X. Huang, S. Zhang, Y. Qi, Z. Liu, J. Nat. Chem. 15 (2006) 38–44.
[33] G. Bonura, M. Cordaro, L. Spadaro, C. Cannilla, F. Arena, F. Frusteri, Appl. Catal. B 140–141 (2013) 16–24.
[34] G. Bonura, F. Arena, G. Mezzatesta, C. Cannilla, L. Spadaro, F. Frusteri, Catal. Today 171 (2011) 251–256.
[35] F. Arena, G. Italiano, K. Barbera, G. Bonura, L. Spadaro, F. Frusteri, Catal. Today 143 (2009) 80–85.
[36] F. Arena, G. Italiano, K. Barbera, S. Bordiga, G. Bonura, L. Spadaro, F. Frusteri, Appl. Catal. A 350 (2008) 16–23.
[37] F. Arena, K. Barbera, G. Italiano, G. Bonura, L. Spadaro, F. Frusteri, J. Catal. 249 (2007) 183–192.
[38] Y.Y. Sun, R. Prins, Angew. Chem. Int. Ed. 47 (2008) 8478–8481.
[39] J. Kim, M. Choi, R. Ryoo, J. Catal. 269 (2010) 219–228.
[40] J. Perez-Ramirez, C.H. Christensen, K. Egeblad, C.H. Christensen, J.C. Groen, Chem. Soc. Rev. 37 (2008) 2530.
[41] Joint Committee Powder Diffraction System, International Centre for Diffraction Data, Swarthmore, USA.
[42] Y. Sun, P.A. Sermon, J. Chem. Soc. Chem. Commun. 16 (1993) 1242.
[43] R.M. Ravenelle, F. Schüßler, A. D'Amico, N. Danilina, J.A. van Bokhoven, J.A. Lercher, C.W. Jones, C. Sievers, J. Phys. Chem. 114 (2010) 19582–19595.
[44] L.H. Ong, M. Dömök, R. Olindo, A.C. van Veen, J.A. Lercher, Microporous Mesoporous Mater. 164 (2012) 9–20.
[45] F. Yaripour, F. Baghaei, I. Schmidt, J. Perregaard, Catal. Commun. 6 (2005) 147–152.
[46] M. Sahibzada, I.S. Metcalfe, D. Chadwick, J. Catal. 174 (1998) 111–118.

Please cite this article in press as: G. Bonura, et al., Catalytic behaviour of a bifunctional system for the one step synthesis of DME by CO_2 hydrogenation, Catal. Today (2013), http://dx.doi.org/10.1016/j.cattod.2013.11.017